DEUTSCHES ELEKTRONEN – SYNCHROTRON **DESY**

DESY 90–153
December 1990

Structure Functions at Small-x: New Physics at HERA

J. Bartels

II. Institut für Theoretische Physik, Universität Hamburg

ISSN 0418-9833

NOTKESTRASSE 85 · 2 HAMBURG 52

To be sure that your preprints are promptly included in the
HIGH ENERGY PHYSICS INDEX ,
send them to the following address (if possible by air mail) :

DESY
Bibliothek
Notkestrasse 85
2 Hamburg 52
Germany

DESY 90-153
December 1990

ISSN 0418-9833

Structure Functions at Small-x: New Physics at HERA

J.Bartels [1]

II. Institut für Theoretische Physik, Universität Hamburg, Germany

ABSTRACT

An review is given of our present understanding of the behavior of deep inelastic structure functions in the small-x region. This includes, in particular, the question how much "new physics" will be seen at HERA.

[1]This paper is based upon talks given at: 25th International Conference on High Energy Physics, Singapore, 2-8 August 1990; XX.International Symposium on Multiparticle Dynamics, Gut Holmecke, Dortmund, 10-14 September 1990; DESY Theory Workshop, DESY, Hamburg, October 1-3, 1990; Large Hadron Collider Workshop, Aachen, 4-9 October 1990; Congressino di Phenomenologia, Perugia, Italy, October 24-26, 1990

1 Introduction

Deep Inelastic scattering of electrons on protons (DIS) (Fig.1) provides the classical test of our parton picture of hadrons and, hence, of QCD at short distances. With the advent of HERA (anticipated for the summer of 1991) as well as the advanced planning of the SSC, LHC and the ep-version LEP-LHC, we are entering new kinematical regions in both $Q^2 = -q^2$ and Bjorken-$x = \frac{Q^2}{2pq}$ (Fig.2). Whereas the large-Q^2 region is expected to exhibit the logarithmic scaling violations predicted by QCD (unless deviations, indicative of new physics in the TeV region, show up), the other direction towards small-x leads to a new kinematic region ,which has not been explored so far and, hence, provides new insight into the dynamics of QCD. Furthermore, estimates indicate that numbers of events at HERA will accumulate at small x: it is therefore mandatory to have a thorough understanding of this kinematic regime. In this talk I will try to summarize, what kind of phenomena we are expecting to see and to what extent we are theoretically prepared. For many details I refer to [1].

Let me briefly recapitulate the set-up. With the variables $Q^2 = -q^2$ and $s = (k+p)^2$ (Fig.1) it is convenient to define, in addition to Bjorken-x, the variable y:

$$y = \frac{2pq}{2pk} \tag{1.1}$$

with

$$Q^2 = xys. \tag{1.2}$$

The Bjorken limit is defined as

$$Q^2 \to \infty, \; x fixed. \tag{1.3}$$

The momentum-transfer Q^2 defines the resolution by which the photon probes the short-distance structure of the nucleon, x is the momentum fraction carried by the struck parton inside the nucleon, and y describes, in the rest frame of the proton, the energy transfer from the incoming to the outgoing electron. For small x we have $\frac{1}{x} \approx \frac{s}{Q^2}$. The connection between different high energy limits is illustrated in

Fig.3, in particular the Bjorken limit and the Regge limit ($s \to \infty, Q^2 \approx Q_0^2$ *fixed*). The small-x region above the Bjorken limit is not far from the Regge limit: it is the continuation of the Regge limit towards large Q^2, and one therefore expects ultimately to face the same dynamics as in the Regee limit. For the discussion of the small-x limit of DIS scattering it is useful to use the variables

$$\xi = \ln\ln\frac{Q^2}{\Lambda^2} \tag{1.4}$$

and

$$y = \frac{8N_c}{\beta_0}\ln\frac{1}{x}. \tag{1.5}$$

As usual, $q(x,Q^2)$ and $g(x,Q^2)$) define the probabilities of finding a quark and a gluon, resp., inside the nucleon. In the naive parton model, the nucleon structure functions F_1 and F_2 are given by:

$$F_1(x,Q^2) = \frac{1}{2}\sum_i Q_i^2 q_i(x,Q^2) \tag{1.6}$$

$$F_2(x,Q^2) = 2xF_1(x,Q^2). \tag{1.7}$$

In QCD, eq.(1.7) no longer holds, since the the longitudinal structure function is nonzero. The differential cross section is:

$$\frac{d^2\sigma}{dxdy} = \frac{4\pi\alpha^2}{Q^2}\left(yF_1(x,Q^2) + \frac{1-y}{y}F_2(x,Q^2)\right). \tag{1.8}$$

Throughout this paper, we shall use F_2, i.e. the momentum-weighted distribution functions. For simplicity, it will be denoted by $F(x,Q^2)$.

The theoretical situation of the various high energy limits shown in Fig.3 can be summarized as follows. The Bjorken limit (in the horizontal direction of Fig.3) is dominated by the light cone behavior of operator products and can therefore reliably be described by perturbation theory [2]. In particular, the renormalization group equation predicts [3,4,5] the Q^2 dependence of the moments of the structure functions. The Regge limit (in the vertical direction of Fig.3), on the other hand, has a strong nonperturbative component: for small momentum transfer scattering of hadrons is dominated by large transverse distances (impact parameter) and, hence, sensitive to the behavior of QCD at large distances. For the moment, no

final solution to the behavior of QCD in this limit is at hand. although important work has been done [6,7,8,9,10,11.12]. In between these two regions lies the small-x limit of deep inelastic scattering: it probes the transition from the perturbative Bjorken limit to the nonperturbative region which extends the Regge limit towards large Q^2, and it thus provides the opportunity to test theoretical ideas about the onset of nonperturbative dynamics in QCD, the change from the language of quarks and gluons to that of composite hadrons.

As it will be descibed below in more detail, this transition does not seem to be an abrupt one but has some "fine structure". Namely, according to the analysis of Gribov, Levin, and Ryskin [13] and Mueller and Qiu [14], there is a strip between the two regions in which, although the standard QCD evolution program is no longer valid, perturbative QCD can still be used. The linear evolution equations of Gribov, Lipatov, Altarelli and Parisi have to be replaced by another set of nonlinear equations, which in the following, I will name GLR-equations. In the derivation of these equations one uses elements of both the Regge limit and the Bjorken limit. When analysing these equations, it turns out that the beginning of the nonperturbative region is marked by a boundary ("critical") line which has the approximate form:

$$y = \frac{1}{4}\exp 2\xi + const. \tag{1.9}$$

The transition across this line appears to be smooth [15]. Due to our lack of a full understanding of the Regge limit, this GLR equation for the intermediate region seems, at present, to be the most useful tool at hand. Further work on its theoretical basis as well as an extended analytic and numerical analysis of its solutions seems most desirable.

This paper will be organized as follows. In the first part (section II) I will try to illustrate, within the parton picture, which modifications have to be included when one moves from the Bjorken limit towards smaller x-values. Then (section III) I turn to a more theoretical description of the small-x region, in particular to the Gribov-Levin-Ryskin equations and the origin of the critical line of Fig.3. In the third part (section IV) I discuss phenomenological aspects: numerical solutions

to these equations and the important question, how HERA can see the beginning of these new facets inside the nucleon.

2 The Parton Picture in the Small-x Region

Let me first recapitulate what goes wrong with the standard QCD evolution program when x is taken to be very small. The small-x behaviour of F_2 is dominated by gluon production and is of the form:

$$F(x,Q^2) \approx \frac{exp\left(\sqrt{2(\xi-\xi_0)y}\right)}{\sqrt{2\pi\sqrt{2(\xi-\xi_0)}}} \tag{2.1}$$

From this it follows that the total cross section for the scattering of a virtual photon off the proton would rise faster than any power of $\ln\frac{1}{x} \approx \ln\frac{s}{Q^2}$. Unitarity, on the other hand, requires that the growth cannot be faster than the square of the hadron radius:

$$\sigma_{tot}^{\gamma^*} = \frac{4\pi^2\alpha}{Q^2}F(x,Q^2) \leq 2\pi R(s)^2, \tag{2.2}$$

and the hadron radius grows as

$$R(s) \approx const \cdot \ln s. \tag{2.3}$$

Somewhere in the small-x region, therefore, the standard QCD description has to become invalid.

That something new has to come in at small values of x can be seen rather easily within the parton picture [13]. The standard QCD-evolution framework can be viewed as a cascade of partonic decay processes inside the nucleon: the photon picks a quark with momentum fraction x and virtuality Q^2 (which is approximately equal to the transverse momentum squared or the inverse square of the transverse radius). Such a quark represents the final result of a chain of subsequent decay processes, in course of which the partons become slower and, at the same time, gain a larger virtuality. This picture is nothing but a space-time interpretation of the QCD-ladder diagrams shown in Fig.4. In the transverse (impact parameter) plane the same situation is illustrated in Fig.5: partons at a low momentum scale

Q^2 (or at the lower end of the ladder) have a rather larger transverse size and are drawn as being "fat" in Fig.5. Partons at the upper end have larger virtuality and are much "thinner" (Fig.5b and c). The number (or density) of the partons is determined by the structure functions: according to eq.(2.1) which represents the "standard QCD evolution", the number of small-x partons increases very fast. Hence, in the transverse plane their density becomes high and it becomes more and more probable that they will interact among each other. In the standard QCD framework, only one type of interaction has been taken into account, namely decay processes which cause the parton density to increase. It therefore appears to be extremely suggestive to expect also other interaction processes, e.g. recombination or annihilation processes which might balance the number of partons or even decrease their density. A possible result of these creation and annihilation processes could be a "saturation" as shown in Fig.6: the "true" QCD structure function no longer increases at small x, it approaches a constant value (up to powers of $\ln\frac{1}{x}$). Such a behaviour would also match the observed slow increase of the hadronic total cross section at low Q_0^2 in the Regge limit. Strong-field calculations within QED and QCD [16] indeed point into this direction.

A simple argument (Fig.7) may illustrate how such partonic annihilation processes will modify the QCD evolution equations. In the standard scenario (Fig.7a) a change of parton densities is obtained by a splitting of the incoming parton into two outgoing partons. Such a change δF is proportional to the probability of finding the initial parton, i.e. we have a linear evolution equation. Recombination processes (Fig.7b), on the other hand, must be proportional to the probability of finding two incoming partons. Most naively, this probability could be assumed to be proportional to the square of the probability of having one parton: one then obtains the nonlinear term indicated in Fig.7b. The strenght of this nonlinear term also depends upon the descent of the two incoming partons: if they originate from one common "parent" parton (e.g. one valence quark), it seems more likely that they have a chance to recombine again than for the case where they come from different valence quarks which are spatially seperated. In the first case, the

strenght would be proportional to the inverse square of the quark radius, in the latter to that of the hadron. Switching back to the language of Feynman diagrams, such a recombination process would be descibed by the (nonplanar) fan diagram shown in Fig.8: taking the energy discontinuity through the center, one obtains the recombination subprocess of Fig.7b. One should, however, note that there are other ways of cutting Fig.8: this indicates that the recombination process of Fig.7b is necessarily accompanied by other processes (rescattering in the initial and final states and diffractive dissociation of the photon).

This very qualitative description of small-x physics allows, in fact, a first estimate of the boundary between perturbative and nonperturbative physics in the ξ, y plane (Fig.2). Consider the quantity

$$W(x,Q^2) = \frac{\alpha_s(Q^2)}{Q^2}\frac{F(x,Q^2)}{R^2} \approx \frac{const}{Q^2 \ln Q^2}\frac{\exp\sqrt{2\xi y}}{y^2} \qquad (2.4)$$

which measures the probability of partons to interact with each other. In order that the standard QCD casacde picture works, this probality should be less than one: neglecting all nonleading terms, this condition can be approximated by

$$y \leq const \cdot \exp 2\xi \qquad (2.5)$$

which is a very crude approximation of the critical line in Fig.3.

To conclude this section, several remarks should be made. First, it has to be emphazised that the use of the parton language for the interpretation of QCD-Feynman diagrams becomes ambiguous if one goes beyond the leading-log Q^2 approximation. It is, therefore, by no means obvious how one could discuss this "new physics" consistently in the parton picture (i.e. without resorting to perturbation theory and Feynman diagrams). For example, it would be very useful to have a more intuitive derivation of the Gribov-Levin-Ryskin equation (which will be discussed below) in terms of partonic subprocesses. This equation is the result of a careful analysis of large classes of Feynman diagrams and takes into account nonleading twist contributions. The simple translation from QCD perturbation theory to the parton picture therefore no longer holds; as an example, one of the

difficulties that one encounters are the so-called Abramovsky-Gribov-Kancheli cutting rules [17], which relate the different energy discontinuities of the fan diagrams to each other.

Second, the inclusion of the new partonic interactions such as annihilations or recombinations can describe only the beginning of new physics ("saturation") in the small-x region: near and beyond the critical line nonperturbative physics sets in, and theoretical progress will necessarily be linked to a better understanding of the nearby Regge limit.

Finally, for practical purposes to be disussed further below it may be necessary to develop a somewhat refined picture of the "saturation" [18]. Whereas the structure functions measure the parton density, averaged over the full transverse size of the nucleon, the saturation of partons may actually begin in a nonuniform fashion (Fig.8). In the simplest scenario, high density of partons may start to develop first close to the valence quarks, whereas other regions inside the nucleon may still remain empty for some range in x. The structure function would then still continue to grow with $\frac{1}{x}$, although locally saturation may have already been reached. Following A.Mueller, one could name these regions "Hot spots". To test this possibility, one has to look for special final states which are designed to probe small areas inside the nucleon. This will be discussed further in the third part of this review.

3 Quantitative Description: QCD and the Gribov-Levin-Ryskin Equation

3.1 General Remarks

After this more qualitative discussion of the small-x region it is necessary to adress the question: how can we make all this more quantitative, e.g. how can we compute these effects and how can we find out for what values of x and Q^2 these new effects start to become important?

It is instructive to first start from the operator expansion and discuss what happens when we approach the small-x limit. It may be useful to remember

that, on very general grounds, moments of the structure function are expected to become singular near n=1: since hadronic total cross sections are slowly growing with energy (presently an increase proportional to $(\ln s)^2$ is observed), a similar behavior is expected for the total cross section for the scattering of a virtual photon off a nucleon. It then follows that the moment

$$\int_0^1 dx x^{n-1} W(x,q^2) = \frac{1}{2\pi} \int_0^1 dx x^{n-1} Im T_{\gamma^* p}(x,q^2) \tag{3.1}$$

should be singular near n=1. Taking the Mellin transform of (3.1), one immediately sees that the small-x behavior of $W(x,Q^2)$ will be dominated by this singular behavior. In perturbation theory this singularity is well-known: the anomalous dimension, e.g., γ_{VV} of the two-gluon operator

$$F^{\alpha\mu_1} D^{\mu_2} ... D^{\mu_{n-1}} F_\alpha^{\mu_n} \tag{3.2}$$

behaves as

$$\gamma_{VV} = \frac{4N}{\beta_0} \frac{1}{n-1} \tag{3.3}$$

near $n = 1$.

Now the important point to note is that this singularity will show up also in gluon operators of higher twists, e.g. in the anomalous dimension of the four-gluon operator:

$$(\partial)^{n_1} A_\mu (\partial)^{n_2} A^\mu (\partial)^{n_3} A_\nu (\partial)^{n_4} A^\nu \tag{3.4}$$

(evolution equations for operators of higher twist have been discussed, for example, in [19]). The usual argument of neglecting, for large Q^2, all operators of twist higher than two, therefore has to be modified in the small-x limit: depending upon the strength of the singularity near $n = 1$ and the smallness of x, operators of higher twist may become as important as or even more important than the twist-two contribution. In general, terms of all twists need to be investigated (i.e. the expansion in inverse powers of Q^2 is no longer useful) , and other arguments have to be used in order to decide which terms have to be kept. I believe that this should be done by starting from the Regge limit where unitarity is the powerful guiding principle, and then approaching the small-x part of the Bjorken limit in

Fig.3 from above, i.e.from the opposite side compared to the perturbative Bjorken limit.

Investigations of the Regge limit of QCD have been started more than ten years ago [6,7,8,9.10,11,12]. One of the strategies starts from a spontaneously broken version of QCD (i.e.giving the gluons a mass allows to avoid infrared problems) and uses perturbation theory to calculate the high energy behavior of elastic and inelastic scattering amplitudes. Since the gluon reggeizes, the analytic structure of the scattering amplitudes has been found to be precisely the same as predicted by S-matrix theory [12], and, as a result, it seems possible to construct a set of high-energy scattering amplitudes which satisfy unitarity in both the s-channel and the t-channel. The actual construction of these amplitudes, however, which has to be based upon dispersion relation techniques, has not yet been carried out. In the next step one has to remove the gluon mass: the fact that the color zero exchange channel seems to be (almost) free of infrared divergencies, whereas amplitudes with color exchange are found to be supressed by infrared divergencies, indicates that these perturbative results are - in some sense - very close to true QCD: they certainly contain the correct short distance part of the (high energy) scattering amplitudes. In the region of small momenta they still seem to represent well-defined expressions, but, most likely, additional (nonperturbative) contributions have to be included (for suggestions in this direction see, e.g. [10,12]). However, it may very well be that the knowledge of the ultraviolet part of the amplitudes is already sufficient to study at least some part of the region above the critical line. For example, it would provide a new derivation of the GLR equation, if one could show that the large-Q^2 limit of the Regge-limit scattering amplitudes agrees with the GLR equation. I shall come back to this a little later.

3.2 The GLR Equation

The first - and so far only - serious attempt for selecting those classes of QCD Feynman diagrams which become important when going from the Bjorken limit towards smaller x-values has been made about ten years ago by Gribov, Levin,

and Ryskin [13] and, somewhat later, by Mueller and Qiu [14]. The first of these corrections to the standard QCD evolution is illustrated in Fig.10. The first term is a repeat of Fig.4, the sum of (gluonic) QCD ladder diagrams which leads to the evolution equations of Gribov, Lipatov, Altarelli, and Parisi. The second part illustrates the first correction (so-called fan diagram): the upper ladder branches into two ladders which at the lower end couple to the nucleon (in our picture only one quark line is shown; other possibilities include the coupling to two different quarks). The branching vertex (triple-ladder vertex) consists of the sum of several (nonplanar) diagrams, only one of which is shown. Taking the energy discontinuity of this set of diagrams in all possible ways, one obtains, among other contributions, the recombination process shown in Fig.7. However, since this set of diagrams allows for other energy cuts, the recombination process in Fig.7 must necessarily be accompanied by other contributions, e.g. the diffractive cut shown in Fig.11. A careful analysis of all these terms leads to the well-known Abramowski-Gribov-Kancheli rules (AGK-rules) [17]. In particular, the sum of all terms carries a minus sign, relative to the ladder diagrams which correspond to the standard evolution equations. Clearly, this minus sign is highly desirable to fight the strong increase of the structure function at small x.

In the approximation where only leading powers in both lnQ^2 and $ln\frac{1}{x}$ are kept (DLA approximation), the behavior of Fig.10 is rather simple. If we denote by $F_0(y,\xi)$ the expression for the right part of Fig.10, then the first correction is given by:

$$-const\int^{y} dy_1 \int^{\xi} d\xi_1 F_0(y-y_1,\xi-\xi_1)V(\xi_1)F_0^2(y_1,\xi_1) \qquad (3.5)$$

where

$$V(\xi) = \frac{3\pi^2}{4\beta_0}\frac{Q_0^2}{\Lambda^2}\exp -e^{\xi} - \xi \qquad (3.6)$$

stands for the triple ladder vertex.

Following Gribov, Levin, and Ryskin, the next corrections beyond the fan diagram of Fig.10 are generalizations indicated in Fig.12: moving from the top to the bottom, QCD ladders branch into two ladders, thus increasing the number of

ladders up to infinity. Diagrams with decreasing number of ladders or diagrams with number-conserving ladder-interaction vertices do not contribute in this transition region. Such contributions are essential in the Regge limit (where it is more appropriate to organize the diagrams in the form of reggeon diagrams), so one might expect that they become important for the small-x limit of DIS as soon as one approaches the critical line. From the point of view of the Regge limit, the fan diagrams of Gribov, Levin, and Ryskin thus represent a subset of the reggeon diagrams which emerge in the Regge limit (to be precise: the ladders appearing in DIS are, for small x, equal to the large-Q^2 limit of the ladder diagrams which appear in the Regge limit). As it was said before, this close connection suggests, as an independent derivation of the GLR equation (or some alternative thereof), to investigate the large Q^2 limit of the reggeon diagrams. This would be the generalization of the well known result [5,20,21] that the large-Q^2 limit of the Lipatov-ladders leads to the singular pieces of the anomalous dimension of the twist-two gluon operator.

In order to proceed further, Gribov, Levin, and Ryskin made an assumption concerning the coupling of $n \geq 2$ ladders to the hadron: this coupling is assumed to be proportional to the n-th power of the single-ladder coupling. As a consequence, the probability of finding two gluons (at low momentum Q_0^2) with momentum fractions x_1 and x_2 is proportional to $g(x_1,Q_0^2)\cdot g(x_2,Q_0^2)$. This assumption then allows to find an equation for the sum of all fan diagrams, the GLR equation. It is a nonlinear integro-differential equation. In its simplest form, the DLA approximation, it is obtained by generalizing eq.(3.5) and performing the sum over all ladders:

$$F(y,\xi) = F_G(y.\xi) - \int_0^y dy' \int_{\xi_0}^{\xi} d\xi' F_0(y-y',\xi-\xi')C\exp(-e^{\xi'}-\xi')F^2(y',\xi'). \quad (3.7)$$

where C stands for the constant factors of (3.6), and F_G denotes the sum of QCD ladder diagrams with some initial distribution $G(y)$. The more accurate form of

the equation is given as:

$$\frac{\partial\phi(x,q^2)}{\partial\ln(\frac{1}{x})} = \int \tilde{K}(q^2,q'^2)\phi(x,q'^2)\frac{4N\alpha_s(q'^2)}{4\pi}dq'^2 - \frac{1}{4\pi R^2}\left(\frac{\alpha_s(q^2)}{4\pi}\right)^2 V\phi^2(x,q^2). \tag{3.8}$$

Here $\phi = \frac{\partial F}{\partial Q^2}$, R denotes the transverse radius of the hadron (or quark), and V stands for the triple ladder vertex, evaluated more accurately than in (3.7), namely in the semiclassical approximation.

As far as I know, there is no real theoretical justification of this assumption: further studies of this point seem to be important.

3.3 Solutions in the Semiclassical Approximation

The first suggestion to solve these nonlinear equations in the semiclassical approximation is again due to Gribov, Levin, and Ryskin [13]. The idea is illustrated in Fig.13. Let me first consider the standard case, the linear evolution equation of Altarelli and Parisi (Fig.13a). According to the evolution equation

$$\frac{\partial G(x,Q^2)}{\partial\ln Q^2} = \frac{\alpha_s(Q^2)}{2\pi}\int_x^1 \frac{dz}{z}P_{gg}(z)G(\frac{x}{z},Q^2) \tag{3.9}$$

we need to know the function $G(x,Q^2)$ at fixed Q^2 for the whole interval (x,1), in order to calculate the change in the Q^2 direction. However, for small x and large Q^2 we really only need knowledge of a smaller and smaller x-interval (for small x, the integral (3.9) is dominated by the lower end of the integration region). This means that the evolution in Q^2 eventually only "propagates" along certain paths in the (Q^2,y) plane which become narrow if we move towards the upper right corner; conversely, in the lower left corner they become more and more diffuse and eventually are "washed out". For the case of the linear evolution equation (3.9) these paths can be shown to be straight lines ("rays"). Their precise intercepts and slopes depend upon the initial conditions of (3.9), i.e.the initial distribution at low Q^2. In any case, each point in the plane can be reached by exactly one ray which starts somewhere in the lower left corner. If we now switch from the linear case (3.9) to the nonlinear case (3.7) or (3.8), this pattern of paths changes (Fig.13b) [15]. In the left upper corner, a region appears which is unaccessible

to trajectories that start in the lower left corner: the boundary line between this "empty" region and its complement is identified with the critical line of Fig.3 and has the characteristics of a caustic line, i.e. it is the envelope to the rays which now are slightly bent. It is the line where the validity of the GLR equation stops: above the line we are in the nonperturbative region which represents the large-Q^2 extension of the Regge limit. Far below this line, the rays are not affected by the nonlinearity, and the linear evolution equations can be used. It is only slightly below the line where the nonlinear term is felt: this is the "intermediate" region alluded to in the introduction. One also finds that at low Q^2 this intermediate region is a narrow strip just below the critical line, and it widens when Q^2 increases. It follows that measurements of the x-distribution of the structure function at rather low Q^2 values will quickly cross the intermediate x-region and enter the nonperturbative domain. As to the position of the critical line, it obviously will depend upon the starting values of the trajectories in the lower left corner, i.e. the initial y-distribution at the low momentum scale Q_0^2. The existence of this critical line is an important feature of the GLR equation: it means that the GLR equation predicts the limit of its validity. The fact that trajectories from the lower left corner never enter the "nonperturbative" part of the plane means that for the description of the "perturbative" region we only need to know the initial y-distribution inside a finite y-interval. All this discussion is based upon a detailed analysis [15] of eq.(3.8) with a particular set of initial conditions, but it is expected that the qualitative picture remains the same for a rather general class of initial distributions. Fig.14 shows some results of this analysis. There may, however, exist also initial distributions for which the character of the critical line of being a caustic is somewhat different [22].

4 Phenomenology

In this final section I adress the question what the chances are to see these effects at HERA. The first topic are numerical solutions of the GLR equation. So far there exist two calculations [15,23]. They both solve eq.(3.7), which can be written also

in another form:

$$\frac{\partial F(y,\xi)}{\partial \xi} = \frac{1}{2}\int_0^y dy' F(y',\xi)(1 - 2C\exp(-e^{\xi} - \xi)F(y',\xi)). \qquad (4.10)$$

This DLA approximation can be valid only for very small x-values. For a realistic numerical estimate it is necessary to improve this approximation. As a first step, one may replace, inside each ladder, the DLA approximation of the splitting function by the full Altarelli-Parisi kernel. Retaining only gluonic contributions one obtains:

$$\begin{aligned}\frac{\partial F(y,\xi)}{\partial \xi} = \frac{1}{2}\int_0^y dy' \Bigg\{ & \frac{z^2 G(y',\xi) - zG(y,\xi)}{1-z} + G(y',\xi)\left[-z + z^2(1-z)\right] \qquad (4.11)\\ & + G(y',\xi)\left[1 - 2C\exp(-e^{\xi} - \xi)G(y',\xi)\right]\Bigg\}\\ & - G(y,\xi)\left[\frac{4N}{\beta_0}\ln(1-x) + 1\right].\end{aligned}$$

Here we defined $z = x/x' = \exp[-(y-y')\beta_0/(8N)]$. This is the improvement used in [15]. In [23] a similar improvement has been used; moreover, the nonlinear equation is applied only above a certain y-value, thus avoiding the problem of the large-x behavior.

As I have explained before, the numerical solution depends upon two input quantities, the initial y-distribution at some low Q_0^2 and the strenght C of the nonlinearity. [15] therefore uses two different input distributions, and both papers vary the parameter C by a factor of 10 or 2.5, resp. Predictions for the (momentum weighted) gluon distribution are shown in Fig.15 -17, for F_2 in Fig.18. In Fig.15, the full curves correspond to the nonlinear evolution: the upper ones to the (steeper) Morfin-Tung initial [24] distribution, the lower ones to the (almost flat) Eichten-Hinchclife-Lane-Quigg [25] distribution. The dashed and the dotted curves show the corresponding results of the standard (linear) evolution programs for two different values of C: the lower curves belong to the larger value (3.9), for the upper ones C is divided by ten. The main point to be emphasized is the fact that e.g. for $Q^2 = 10GeV^2$, deviations are visible already at x close to 10^{-2}. For the larger of the two C-values this effect is, of course, more pronounced than for the smaller one. Fig.16 shows lines of fixed deviations of the linear from the non-

linear evolution: the dashed-dotted line is the critical curve of Levin and Ryskin [26]:

$$Q_c^2(x) = Q_0^2 - A^2\exp(3.56\sqrt{\ln\frac{1}{x}}) \qquad (4.12)$$

with

$$A = 52MeV \quad Q_0^2 \quad 2GeV^2 \qquad (4.13)$$

Again, the point to be stressed is the fact that deviations are sizable at not so small x. An analysis analogous to Fig.14 has not yet been done for this model. Figs.17 and 18 show results of [23] for $xg(x,Q^2)$ and $F_2(x,Q^2)$, resp. In this case the input distribution is again a rather steeply rising function in y; its analytic form has been motivated by the analysis of [27]. Deviations between the linear and the nonlinear evolution start at x between 10^{-2} and 10^{-3}, quite in agreement with the findings of [15]. [23] also presents results for F_2: it is, however, not clear whether this calculation takes into account certain difficulties which have been pointed out in [28]: once the gluon structure function has been calculated from the GLR-equation, the quark loop which couples the gluons to the deep inelastic photon, can no longer be used in the leading-Q^2 approximation.

The important message of these two papers seems to be that, provided the x-distribution at low Q^2 is as steeply rising as it was assumed in most of these calculations, HERA will enter the region where the "new" physics is at work. To be more precise, since at these relatively small values of $Q^2 \approx 10GeV^2$ the "intermediate" region between perturbative and nonperturbative QCD is very narrow, HERA not only enters this transition region but also reaches into the domain of nonperturbative QCD. Here, strictly speaking, we have no reliable theory. As a first estimate, one might try to use the solution of the GLR equation: it predicts saturation [27] and thus avoids the obvious conflict with s-channel unitarity. It should, however, be repeated that this equation does not claim to be applicable in the nonperturbative region and, hence, cannot be taken as describing the "true QCD behavior". Again, what is lacking is the analysis of the Regge limit of QCD.

The other remark that has to be made concerns the question whether it is

possible to conclude from HERA measurements beyond any doubt, whether one sees this new physics or not. Due to our ignorance of the correct x-distribution at low Q_0^2 which always enters the calculation as an input, it is very well possible that the measurement of some flatter structure function can be descibed by the standard evolution, using some modified input function. Conversely, a continuing rise of the structure function at low x is not necessarily a reliable indication that the "new physics" is not yet at work.The best way to distinguish is the comparison of evolution in Q^2: linear and nonlinear evolution equations predict different Q^2-dependence. In order to extract this from data we need: (i) a range in Q^2 as large as possible and (ii) computer algorithms for both the linear and the nonlinear evolution equations. Whether HERA will satisfy the first requirement, is not yet clear to me. As to the second demand, more theoretical work is necessary, both for the analytic analysis of the GLR equation and for numerical solutions.

Because of these difficulties it is inevitable to look for experiments which are specially designed to probe the "new physics". So far, two such experiments have been proposed. The one is due to A.Mueller [16] and refers to the "hot spots" mentioned before, the other uses the diffractive dissociation of the photon and has been proposed by Ryskin [26]. At the end of section II I mentioned the possibility that "saturation" of soft gluons may set in nonuniformly, i.e. there may be regions inside the nucleon (Fig.5) which are more densely populated by soft gluons than others. Since the structure function F_2 ("total photon hadron cross section") measures the parton density, averaged over the full size of the hadron, one needs to look at exclusive final states which measure the distribution of partons inside limited subregions of the hadron (Fig.5b). Such an experiment is illustrated in Fig.19: measure the cross section of jets which carry the momentum fraction x (not to be confused with the usual Bjorken x_B which belongs to the photon at the upper end) and the momentum scale (transverse momentum squared) $k_\perp^2$. The latter should be not much smaller than Q^2; the mass of the photon: $R_{parton}^2 \approx \frac{1}{Q^2}$ is the transverse radius of the parton struck by the photon, and $R_{jet}^2 \approx \frac{1}{k_\perp^2}$ is the square of the average transverse distance, by which the parent-gluon of the jet is

seperated from this parton. If $k_\perp^2 \leq Q^2 \ll Q_0^2$, then $R_{parton}^2 \leq R_{jet}^2 \ll R_{hadron}^2$, and this process explores the parton cloud of diameter R_{jet} around the struck parton. The cross section should be measured as a function of the ratio $\frac{x_B}{x}$, and the region of interest is where $x_B \ll x$. The cross section for this process is, in the QCD-parton model, given by:

$$\frac{k_\perp^2 x d(\nu W_2}{dx dk_\perp^2} = C\alpha(Q^2)\left(xg(x,k_\perp^2) + \frac{4}{9}(xq(x,k_\perp^2) + x\bar{q}(x,k_\perp^2))\right) F(\frac{x_B}{x}, Q^2, k_\perp^2) \tag{4.14}$$

where C is a normalization factor, $q(x,q^2)$ and $g(x,q^2)$ are the quark and gluon distribution functions, resp., and $F(\frac{x_B}{x}, Q^2, k_\perp^2)$ stands for the sum of QCD ladders above the jet, evaluated in the limit $\frac{x_B}{x} \to 0$ (this is one of the places where the so-called "Lipatov Pomeron" [10] could be tested). This formula predicts a steep rise as $\frac{x_B}{x}$ becomes small:

$$F(\frac{x_B}{x}, Q^2, k_\perp^2) \approx C\frac{\exp\left(\frac{12\alpha(Q^2)}{\pi}\ln 2 \ln\frac{x}{x_B}\right)}{\sqrt{\ln\frac{x}{x_B}}} \tag{4.15}$$

and a deviation from this would be indicative of "local saturation", i.e. the existence of a "hot spot". Corrections to this formula can (and should) be calculated: these are not fan-diagrams but reggeon diagrams, since both Q^2 and $k_\perp^2$ are of the same order. Eq.(4.14) has not been evaluated numerically: this will clearly be necessary in order to estimate the number of events and the event structure.

Another strong prediction based upon the existence of such "hot spots" has been made by Ryskin [29]. Instead of the "one-jet inclusive cross section" of Fig.19 one considers the photon diffractive dissociation processes shown in Fig.20 (its connection with the Pomeron structure function [31,32,33] has been discussed in [30]): there is a rapidity gap between the proton at the lower end and the missing mass cluster above. As an example, this missing mass final state could consist of three jets, originating from $q\bar{q}g$. The final states are further restricted by the requirement that the jet in the direction of the Pomeron should have a controllable $k_\perp$. It is then the dependence upon this $k_\perp$ which distinguishes between "saturation" and "standard" QCD behavior: with saturation the cross section

should be substantially smaller, and for the integrated cross section there could be a difference up to a factor of one hundred!.

There are clearly more measurements that might be suitable to test the presence of the "new physics" described in this talk: this will not be discussed here and should be a topic of further theoretical work.

5 Summary

This talk tried to describe our present understanding of the small-x behavior of deep inelastic structure functions in QCD, partially as preparation for HERA experiments which are expected to start in 1991, partially in order to stimulate further theoretical efforts towards studying QCD at the interface between perturbative and nonperturbative high energy limits.

From the theoretical viewpoint, the low-x region in deep inelastic scattering describes the transition from perturbative to nonperturbative QCD. In the former region we have the well-tested evolution equations of Gribov, Lipatov, Altarelli, and Parisi, whereas for the nonperturbative small-x limit which is the large-Q^2 continuation of the Regge limit we do not yet know what QCD predicts. In between these two regions, however, there is an intermediate regime, for which Gribov, Levin, and Ryskin suggested a new, nonlinear evolution equation which is still based upon perturbative QCD. Although its validity in the x-Q^2 plane is limited and does not extend into the nonperturbative region, its predictions for this region are consistent with unitarity and, in particular, the idea of "saturation". The theoretical basis of this equation lies in the analysis of classes of Feynman diagrams: since it is such an important equation (and also relies on a few assumptions which need further justification!), it seems inevitable to look further into the derivation of this equation (or to find alternatives).

More general, the theoretical investigation of the transition from perturbative to nonperturbative QCD seems to offer an excellent opportunity for testing ideas on confinement dynamics in QCD: when approaching, at some large Q^2, smaller and smaller values of x, interactions between the (initially free) partons become

more and more frequent. Beyond a certain point in x, one seems to reach a state in which a description in terms of partonic degrees of freedom is no longer useful, and one has to switch to hadronic degrees of freedom. To follow this transition in more detail, appears to be the theoretical challenge.

The analysis of the GLR equation has just been started: apart from attempts to use the semiclassical approximation for an analytic solution, only two numerical computer calculations are available. In contrast to the standard linear evolution equations, the nonlinearities make the calculations much more difficult. The numerical results mark the strong dependence of the results on the (unknown) input distribution and on the (unknown) strenght of the nonlinearity. Correspondingly, there is a principal uncertainty where (in x and Q^2) these new effects become relevant. Moreover, even if we are in the right regime, this uncertainty is also likely to make the interpretation of experimental data difficult: if deviations from the small-x prediction of some parametrization of structure functions are observed, it may happen that these effects can be compensated by a change of the input distribution and/or the strenght of the nonlinearity. Measuring not only the x-distribution at some fixed Q^2 but also the Q^2-evolution of the structure function in the small-x region will certainly be of help.

This makes it mandatory to look for other measurements which test the onset of this "new physiscs" more directly. Such experiments have been proposed, but they need more theoretical preparation.

One of the most important questions of practical relevance is the location in the x-Q^2 plane of the transition from perturbative to nonperturbative QCD. At present the most reliable estimates come from the two numerical evaluations of the GLR equation, but as it was said before, there is the uncertainty due to the input parameters. Both calculations indicate that HERA will enter this transition region, and, at low Q^2, even reach into the nonperturbative domain where the parton picture no longer holds.

Acknowledgements

I have profitted very much from discussions with J.Bluemlein, G.Ingelman, E.Levin, L.Lipatov, A.Mueller, O.Nachtmann, M.Ryskin, and G.Schuler.

References

[1] *Proceedings of the Small-x Workshop*, held at DESY, May 1990 (to be published in *Nucl.Physics*, ed.A.Ali and J.Bartels);

[2] For general reviews on perturbative QCD see, e.g.: H.D.Politzer, *Phys.Rep.* **14C**, 129(1974); C.H.Llewellyn Smith, Schladming Lectures 1987, *Acta Phys.Austr. Suppl.XIX*, 331(1978); Yu.Dokshitzer, D.I.Dyakonov, S.I.Troyan, *Phys.Rep.* **58**, 269(1980); E.Reya, *Phys.Rep.* **69**, 195(1981); A.H.Mueller, *Phys.Rep.* **73**, 237(1981); G.Altarelli, *Phys.Rep.* **81**,1 (1982).

[3] V.N.Gribov and L.N.Lipatov, *Sov.Journ.Nucl.Phys.* **15**, 438 and 675 (1972).

[4] G.Altarelli and G.Parisi, *Nucl.Phys.* **126**, 297(1977).

[5] Yu.L..Dokshitser, *Sov.Phys.JETP* **46**, 641(1977).

[6] E.A.Kuraev, L.N.Lipatov, V.S.Fadin, *Sov.Phys.JETP* **44**, 443(1976).

[7] E.A.Kuraev, L.N.Lipatov, V.S.Fadin, *Sov.Phys.JETP* **45**, 199(1977).

[8] Ya.Ya.Balitzky, L.N.Lipatov *Sov.Jour.Nucl.Phys.* **28**, 822(1978).

[9] Ya.Ya.Balitzky, L.N.Lipatov *JETP Letters* **30**, 355(1979).

[10] L.N.Lipatov, *Sov.Phys.JETP* **63**, 904(1986) and references therein.

[11] J.Bartels, *Nucl.Phys.* **B151**, 293(1979); *Nucl.Phys.* **175**, 365(1980); *Acta Phys.Pol.* **B11**, 281(1980); unpublished.

[12] A.R.White, ANL-HEP-PR-90-28 and references therein.;

[13] L.V.Gribov, E.M.Levin, and M.G.Ryskin, *Phys. Rep.* **100**, 1 (1982)

[14] A.H.Mueller and J.Qiu, *Nucl.Phys.* **B268**, 427 (1986).

[15] J.Bartels, J.Blümlein, G.Schuler, DESY 90-91 and to appear in Zeitschr.f.Physik C.

[16] A.H.Mueller, *Nucl.Phys.* **B307**, 34 (1988); *Nucl.Phys.* **B317**, 573(1989); *preprint Columbia Univ.* **CU-TP-441**.

[17] V.A.Abramovsky, V.N.Gribov, O.V.Kancheli,*Sov.Journ. Nucl.Phys.* **18**, 595(1973).

[18] A.H.Mueller, to appear in the *Proceedings of the Small-x Workshop*, held at DESY, May 1990 (to be published in *Nucl.Physics*, ed.A.Ali and J.Bartels);

[19] A.P.Bukhvostov, G.V.Frolov, L.N..Lipatov, *Nucl.Phys.* **B258**, 601(1986).

[20] T.Jaroscewicz, *Phys.Lett.* **116B**, 291(1982).

[21] J.C.Collins, J.Kwiecinsky, *Nucl.Phys.* **B316**, 307(1988).

[22] E.M.Levin and M.G.Ryskin, private communication.

[23] J.Kwiecinski, A.D.Martin, W.J.Stirling, and R.G. Roberts, Rutherford Preprint RAL-90-053

[24] J.Morfin and Wu-Ki Tung, preprint Fermilab–Pub 90/74 (1990).

[25] E. Eichten et al., Rev. Mod. Phys. **56** (1984) 579 and Erratum **58** (1986) 1065.

[26] M.G.Ryskin, *Sov.Journ.Nucl.Physics* **47**, 230 (1988).

[27] J.C.Collins, J.Kwiecinsky, *Nucl.Phys.* **B335**, 89 (1990).

[28] E.M.Levin and M.G.Ryskin, Frascati Preprint April 1990.

[29] M.G.Ryskin, DESY 90-050 and to appear [1].

[30] J.Bartels, G.Ingelman, *Phys.Lett.* **235B**. 175 (1990).

[31] G.Ingelman and P.Schlein, *Phys.Lett.* **152B**, 256(1985).

[32] H.Fritzsch and H.H.Streng, *Phys.Lett.* **154B**, 391(1985).

[33] E.L.Berger, J.C.Collins, D.E.Soper, G.Sterman, *Nucl.Physics* **B286**, 704 (1987).

Figure Captions

Fig. 1: Kinematics of deep inelastic scattering

Fig. 2: Kinematic regions of HERA and LEP/LHC (only for $Q^2 > 3GeV^2$)

Fig. 3: Different High Energy Limits

Fig. 4: QCD ladder diagrams describing the standard linear QCD evolution equation of the gluon structure function (quark contributions are left out).

Fig. 5: Partons in the transverse plane (impact parameter plane)

Fig. 6: Small-x behavior of the structure function: standard QCD evolution versus"true QCD" evolution: region A is the perturbative region, B the transition region, and C the nonperturbative region.

Fig. 7: Partonic subprocesses: (a) splitting of partons (b) partonic recombination process

Fig. 8: Schematic view of QCD diagrams which contain the recombination process of Fig.7b (fan digram)

Fig. 9: A "Hot spot" in the transverse plane

Fig. 10: QCD ladders (a) and the first correction, the so-called fan diagram (b)

Fig. 11. Diffractive cut through the first fan diagram: it leads to the photon diffractive dissociation process discussed in Section IV.

Fig. 12: The sum of fan diagrams which form the basis of the Gribov-Levin-Ryskin equation

Fig. 13: Semiclassical paths of evolution in the x-Q^2 plane: (a) the linear case, (b) the nonlinear case.

Fig. 14: The same as in Fig.13: results from a computer analysis (from [15]). In the third figure we show trajectories in the "nonperturbative" region: they do not cross the "critical" between the two regions.

Fig. 15: x-distributions of $xg(x,Q^2)$ for the model of [15] for different values of Q^2. The full lines belong to the linear equation ($C = 0$), the dashed ones to the nonlinear case with C of eq.(2.3), and the dotted ones to the nonlinear case with $\frac{1}{10}C$. In each case, the upper curves belong to the steeper input distribution, the lower ones to the flat input.

Fig. 16: Comparison of the linear and the nonlinear evolution equations in [15]: the drawn (dotted, dashed) lines indicate where the result of the linear equation differs from the nonlinear one by 10%(20%, 50%). The line marked by "LR" corresponds to eq. (5.4) and denotes the critical line of Levin and Ryskin.

Fig. 17: x-distributions of $xg(x,Q^2)$ for different values of Q^2 (from [23]): the solid line belong to the linear evolution. The dashed and the dot-dashed lines are the results of the nonlinear evolution; in the second case the nonlinearity parameter is increased by a factor of 2.5, compared to the first one.

Fig. 18. x-distributionsfor $F_2(x,Q^2)$ (from [23]): for the upper three curves the notation is the same as for Fig.17. The dotted curve corresponds to another input distribution (which is flat for $x \to 0$).

Fig. 19: A final state configuration which probes the "Hot spot"

Fig. 20: Final state configuration for photon diffractive dissociation

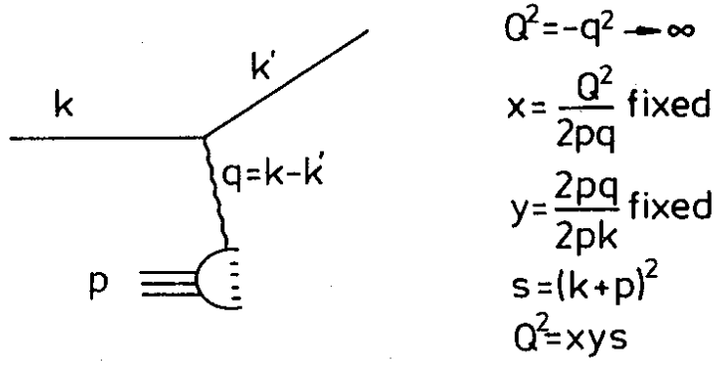

Fig. 1

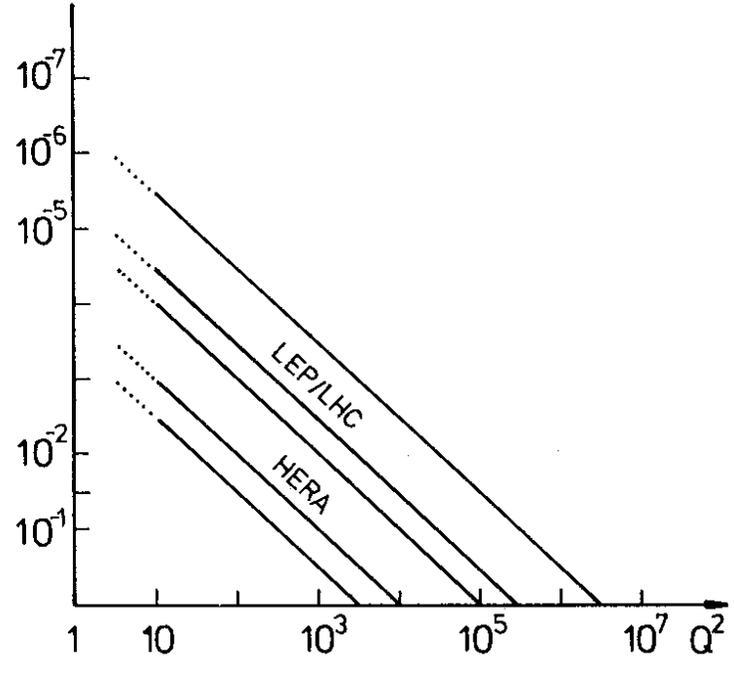

Fig. 2

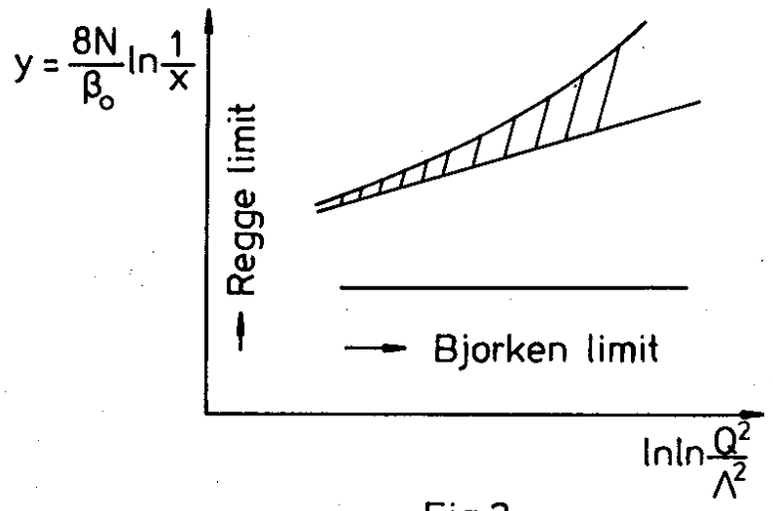

Fig.3

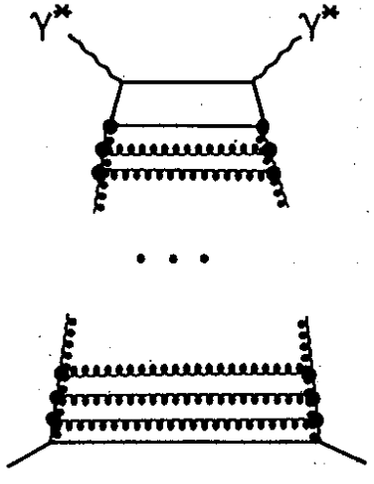

Fig.4

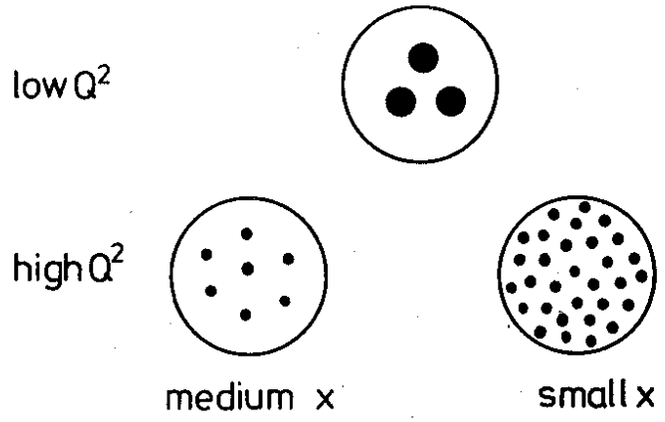

Fig.5

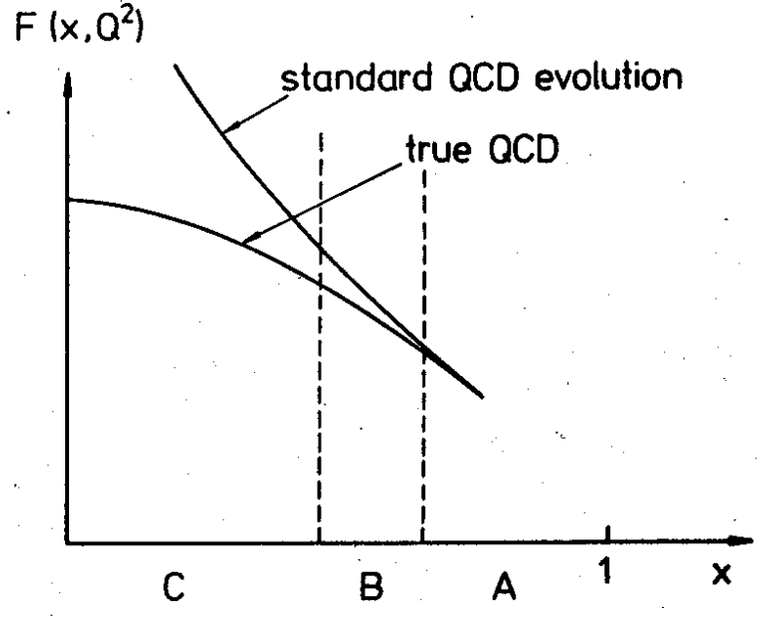

Fig.6

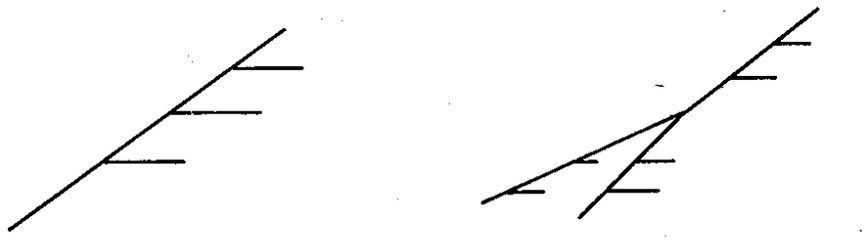

(a) Standard: splitting (b) New: recombination

Fig.7

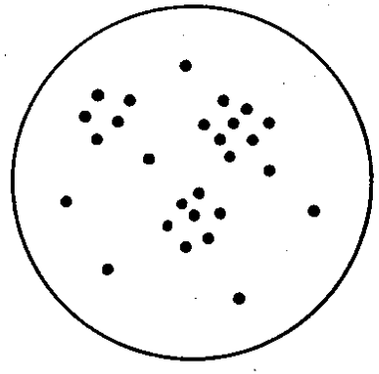

Fig.9

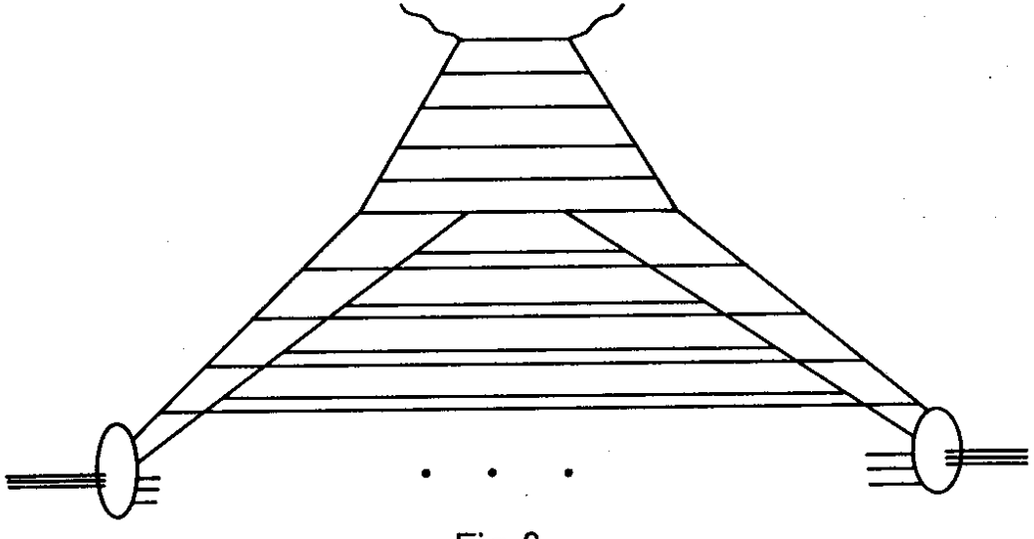

Fig. 8

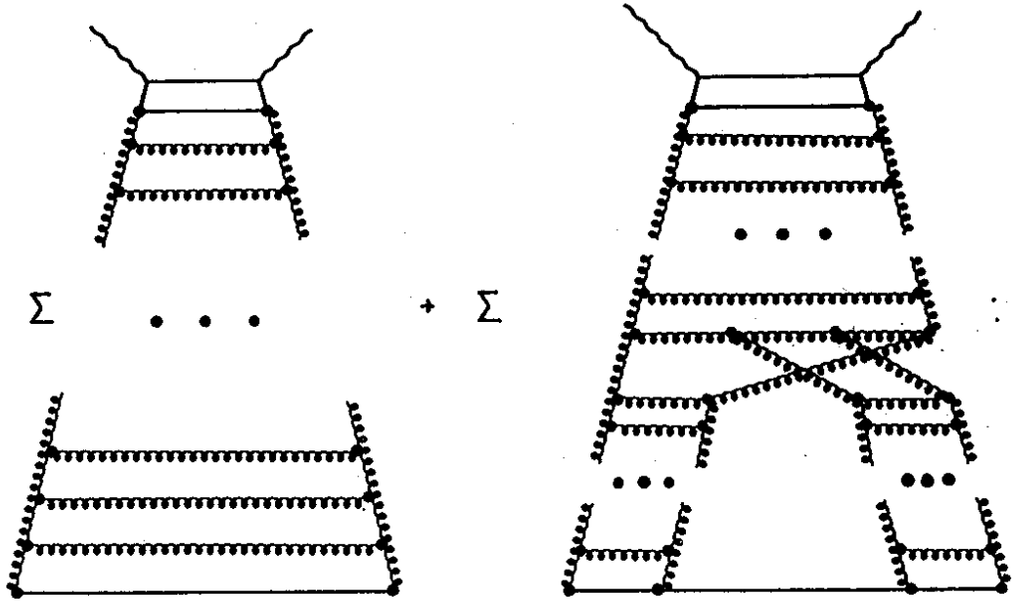

Standard (a)

First correction (b)

Fig.10

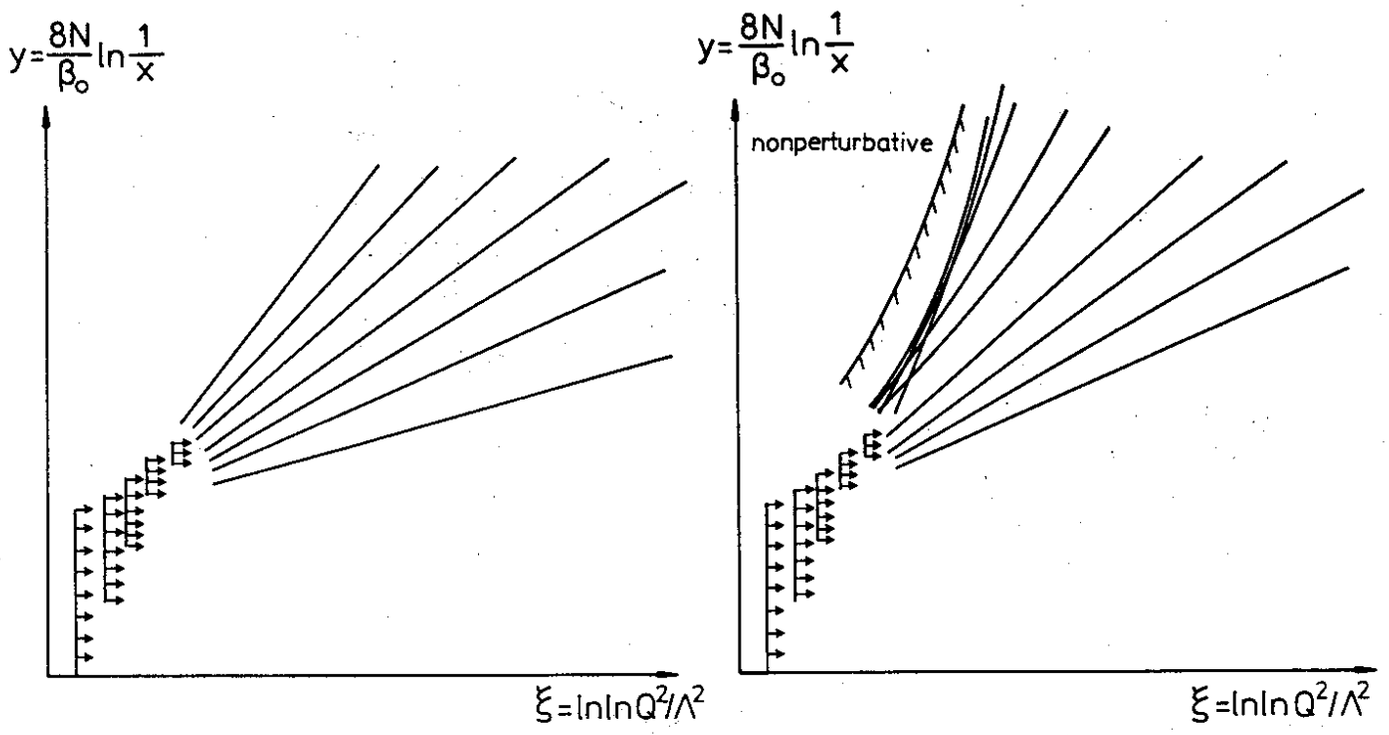

Fig. 13

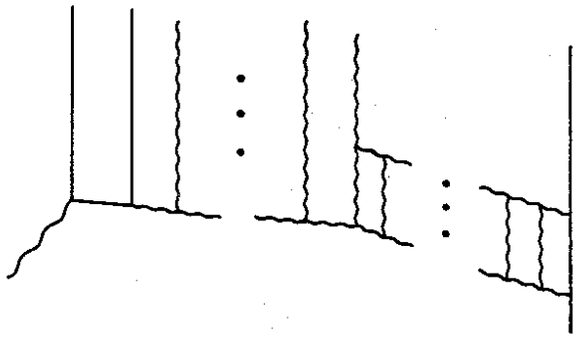

Fig.11

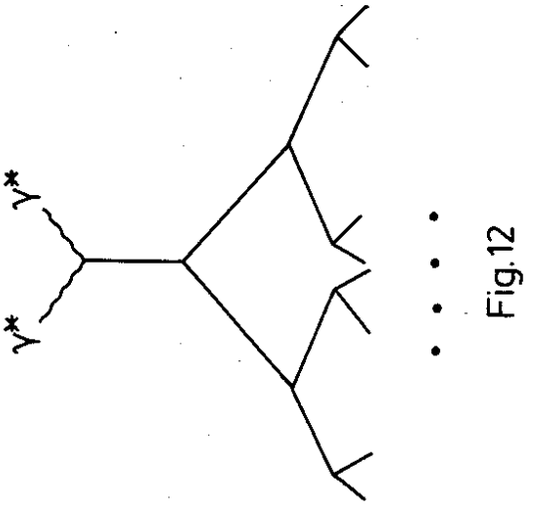

Fig.12

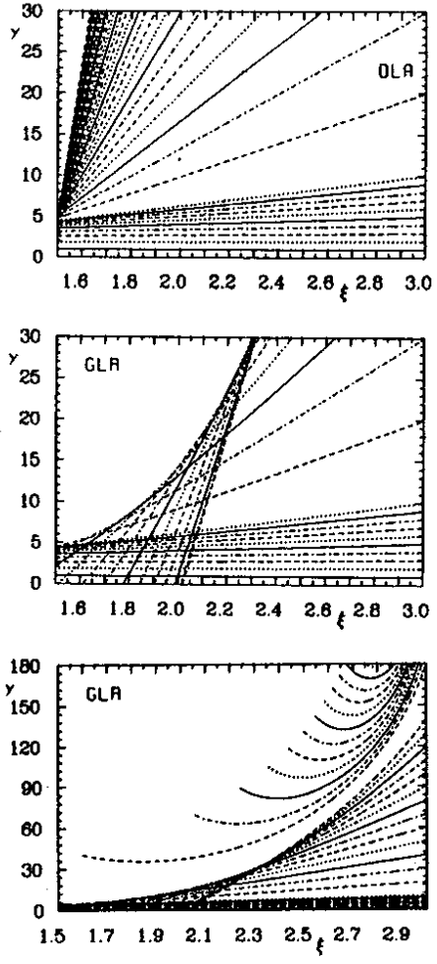

Fig.14

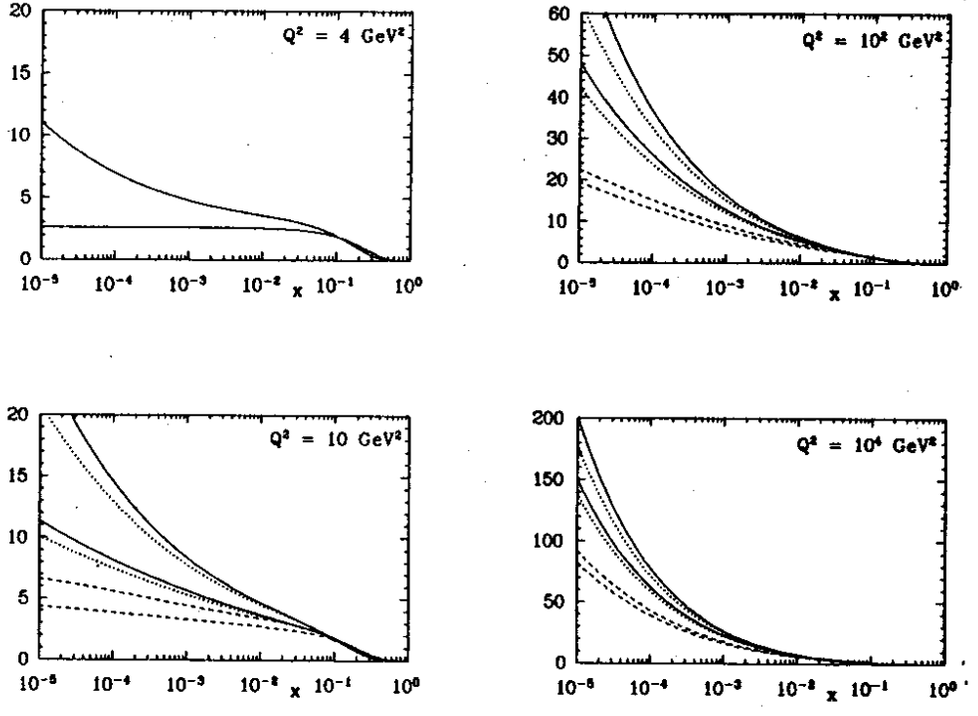

Fig.15

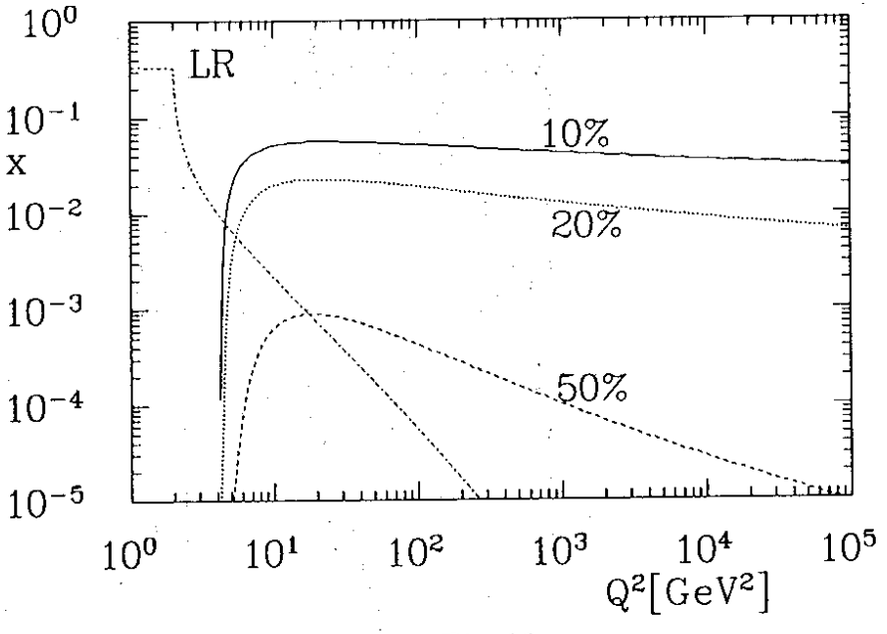

Fig.16

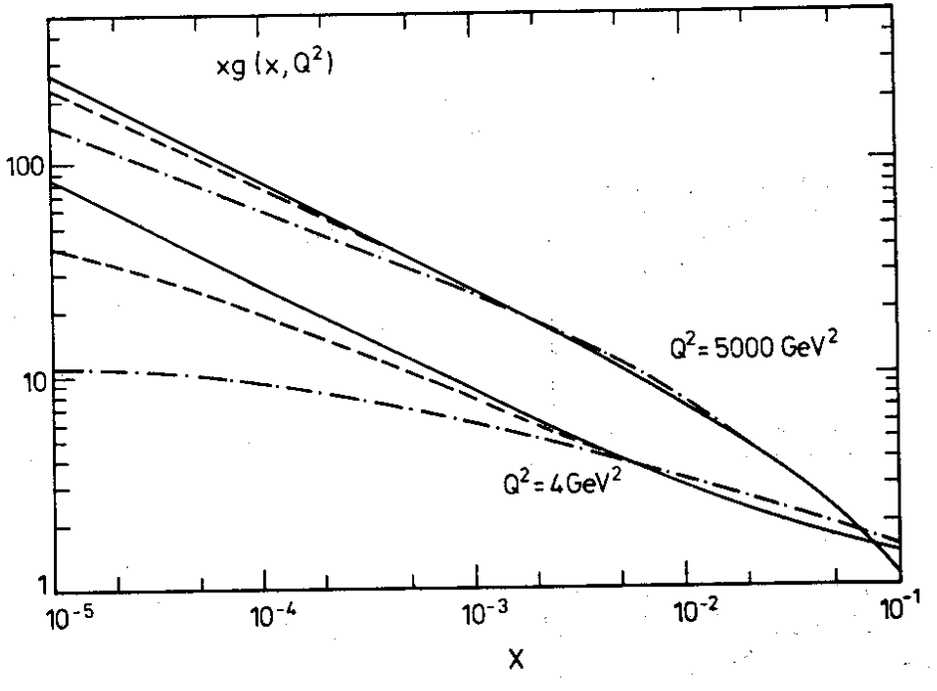

Fig. 17

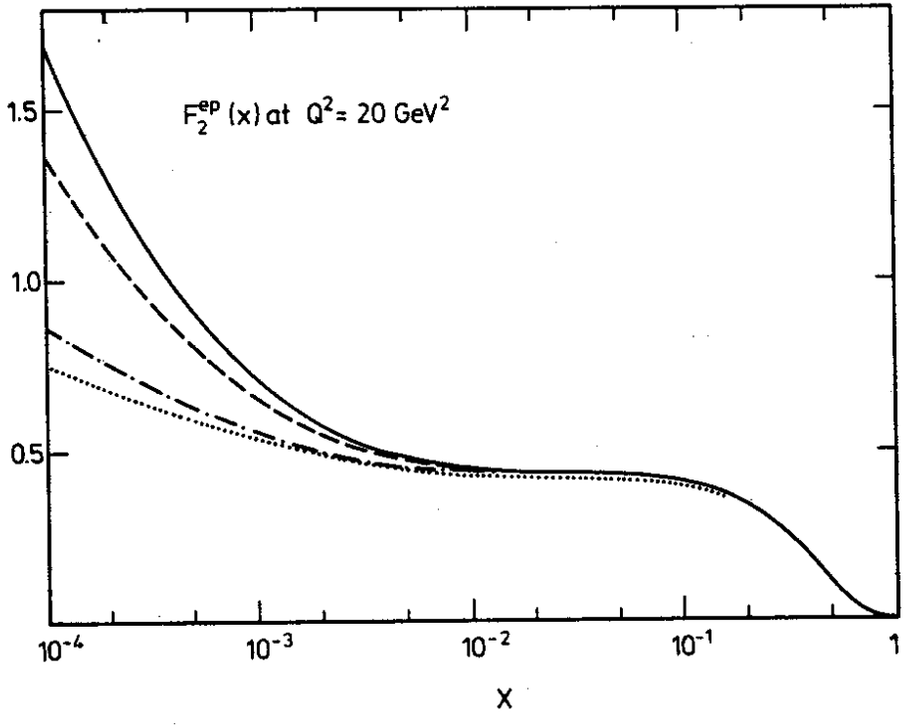

Fig. 18

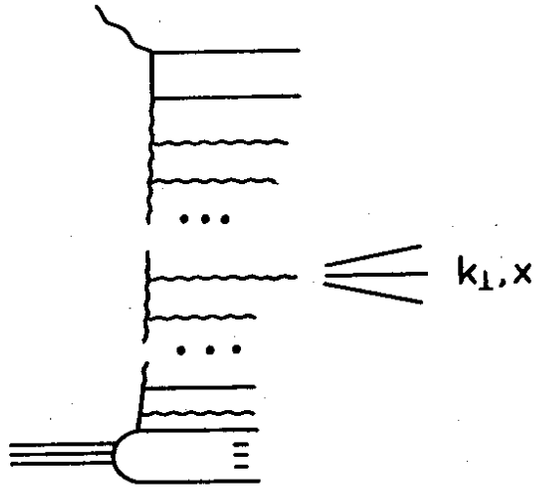

Fig. 19

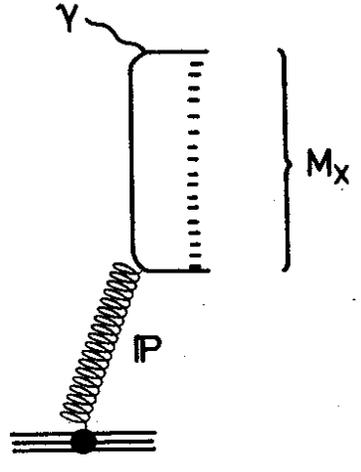

Fig. 20